J. Am. Chem. Soc. 1984, 106, 3844-3850

Synthesis and Conformational Studies by X-ray Crystallography and Nuclear Magnetic Resonance of *cyclo*(L-Phe-L-Pro-D-Ala)$_2$

Gopinath Kartha,*† K. Krishna Bhandary,† Kenneth D. Kopple,*‡ Anita Go,‡ and Peng-Peng Zhu‡

Contribution from the Biophysics Department, Roswell Park Memorial Institute, Buffalo, New York 14263, and the Department of Chemistry, Illinois Institute of Technology, Chicago, Illinois 60616. *Received August 22, 1983*

Abstract: *cyclo*(Phe-Pro-D-Ala)$_2$, $C_{34}H_{42}N_6O_6$, was synthesized from the hydrochloride of Pro-D-Ala-OMe. NMR data indicate that the two-cis backbone is the major form in solution. Crystals were obtained from a solution of the peptide in a mixture of Me_2SO and water and have two molecules in the asymmetric unit of a monoclinic cell with a = 18.730 (2) Å, b = 9.239 (1) Å, c = 21.544 (2) Å, β = 95.17 (2)°, and space group $P2_1$. Both molecules have nearly identical conformation and each contain two cis Phe-Pro bonds. There are no intramolecular hydrogen bonds or β turns. The close similarity in the overall backbone conformation of the two independent molecules in the crystal suggests that the conformation in solution is probably the same as that in the crystal. NMR studies confirm this suggestion. The NMR studies included nuclear Overhauser enhancement measurements on solutions in sulfolane, a more viscous solvent chosen to increase the effective rotational correlation time. Evidence indicating a similar solution conformation for the two-cis form of *cyclo*(Leu-Pro-D-Ala)$_2$ is given.

Many cyclic hexapeptides of the sequence *cyclo*(Xxx-Pro-Yyy)$_2$ have been studied by nuclear magnetic resonance methods.[1] They provide convenient models in which to examine sequence and solvent effects on peptide conformation in a limited region of conformation space.[1-3] The subset of these peptides with the sequence *cyclo*(Xxx-Pro-D-Yyy)$_2$ has been found usually to exist in two forms of average C_2 symmetry, which differ in whether the Xxx-Pro peptide bonds are trans or cis[1,2,4] although unsymmetrical forms have recently been found for some examples.[5] The principal factors identified as influencing the position of the two-cis, all-trans equilibrium are the transannular electrostatic or hydrogen bonding interactions among the N—H and C═O units of the Xxx residue and crowding of the Xxx side chain and the δ-CH_2 of Pro, both of which occur in the all-trans form and have been presumed absent or reduced in the two-cis form.[2,4]

Three examples in which all of the peptide bonds are trans have been analyzed by single-crystal X-ray diffractometry, *cyclo*-(Gly-Pro-D-Phe)$_2$,[6] *cyclo*(Ala-Pro-D-Phe)$_2$,[7] and *cyclo*(Gly-Pro-D-Ala)$_2$.[8] These all show very much the same conformation, a backbone based on two Type II Pro-D-Yyy β turns that is also definitively identified in solution by NMR studies. Past NMR studies of the form with two cis Xxx-Pro bonds have not yielded sufficient evidence for an unequivocal statement about its conformation, and until now no crystal of a two-cis form has been subjected to X-ray analysis.

We have now obtained crystals of *cyclo*(Phe-Pro-D-Ala)$_2$, hereafter PPA2, in which the two-cis form occurs, and we report here its crystal structure. We also report NMR measurements including nuclear Overhauser enhancements that confirm that the solution conformation, in which transannular interactions between CO-NH units are absent, is like the conformation in the crystal. The crystal of PPA2 used contained water held in channels between hydrophobically packed peptide units in a manner similar to that found for the hydrophobic decapeptide antamanide.[9]

Experimental Section

***cyclo*(Phe-Pro-D-Ala)$_2$** was prepared starting from the hydrochloride of Pro-D-Ala-OMe.[10] This dipeptide was coupled with benzyloxycarbonyl-L-phenylalanine *N*-hydroxysuccinimide ester in dimethylformamide (DMF) solution. Half of the resulting tripeptide ester was converted to hydrazide by treatment with hydrazine in methanol, and half was hydrogenolyzed in methanol (Pd on carbon) to the N-unblocked tripeptide ester. The two portions were coupled via the azide in DMF to form the protected hexapeptide ester, which was hydrazinolyzed, hydrogenolyzed, and finally cyclized in DMF via the azide procedure at about 4 × 10^{-3} M. The procedures have been described in detail elsewhere for other peptides.[4] Intermediates were isolated free of peptide or peptide-like impurities according to thin-layer chromatography, but they were not crystallized for analysis. The cyclic hexapeptide was readily isolated from the cyclization reaction mixture by evaporation of the solvent and sonication of the residue with water until it crystallized. It was twice recrystallized from 2-propanol and obtained in 25% yield from the dipeptide starting material. The yield of the cyclization step itself was 51%. An analytical sample was dried at 100 °C under vacuum overnight and decomposed above 300 °C without melting.

Anal. Calcd for $C_{34}H_{42}N_6O_6$: C, 64.74; H, 6.71; N, 13.33; Found: C, 64.49; H, 6.67; N, 13.20.

X-ray Crystallography. Well-formed crystals were grown from a solution of PPA2 in Me_2SO and water. The crystals were stable outside the mother liquor. A crystal of dimensions 1.6 × 0.8 × 0.3 mm mounted on a glass fiber was used for data collection. Unit cell dimensions and intensity data were obtained with an Enraf-Nonius CAD4 atomatic diffractometer. The cell parameters were measured by the least-squares fit using 25 reflections. PPA2 crystallizes in a monoclinic unit cell of dimensions a = 18.730 (1) Å, b = 9.239 (1) Å, c = 21.544 (2) Å, and β = 95.11 (2)°. There are four molecules in the unit cell of space group $P2_1$ with a volume of 3713 A^3.

Intensity data up to 2θ = 154° were measured by using Cu K_α (λ 1.5418 Å) by the ω–2θ scan technique. During the course of data collection three reflections monitored every 2 h indicated no crystal deterioration. A total of 8857 unique reflections were measured of which 7765 were above $3\sigma(I)$, and these were used in structure determination and refinement. The intensity data were corrected for Lorentz-polarization effects and absorption.

The structure was solved by using the direct methods program MULTAN 80.[11] After repeated trials 160 phase sets generated by using 488

(1) Gierasch, L. M.; Deber, C. M.; Madison, V.; Niu, C.-H.; Blout, E. R. *Biochemistry* **1981**, *20*, 4730-4738.
(2) Kopple, K. D.; Sarkar, S. K.; Giacometti, G. *Biopolymers* **1981**, *20*, 1291-1303.
(3) Kopple, K. D.; Zhu. P.-P.; Go, A. *Biopolymers* **1983**, *22*, 153-156.
(4) Kopple, K. D.; Schamper, T. J.; Go, A. *J. Am. Chem. Soc.* **1974**, *96*, 2597-2605.
(5) Kopple, K. D.; Parameswaran, K. N. *Int. J. Pept. Protein Res.* **1982**, *21*, 269-280.
(6) Brown, J. N.; Yang, C.-H. *J. Am. Chem. Soc.* **1979**, *101*, 455-459.
(7) Brown, J. N.; Teller, R. G. *J. Am. Chem. Soc.* **1976**, *98*, 7665-7669.
(8) Kostansek, E. C.; Lipscomb, W. N.; Thiessen, W. E. *J. Am. Chem. Soc.* **1979**, *101*, 834-837.
(9) Karle, I. L. In "Peptides, Proceedings of the 6th American Peptide Symposium"; Gross, E., Meienhofer, J., Eds.; Pierce Chemical Co.: Rockford, IL, 1979; pp 681-690.
(10) Nicolaides et al. (Nicolaides, E.; Dewald, H.; Westland, R.; Lipnik, M.; Posler, J. *J. Med. Chem.* **1968**, *11*, 74-79) report the preparation of Z-Pro-D-Ala-OMe, the precursor of the amino component, but no analysis. Our preparation had mp 90-92 °C. Anal. Calcd for $C_{17}H_{22}N_2O_5$: C, 61.06; H, 6.63; N, 8.38. Found: C, 61.01; H, 6.64; N, 8.33.

† Roswell Park Memorial Institute.
‡ Illinois Institute of Technology.

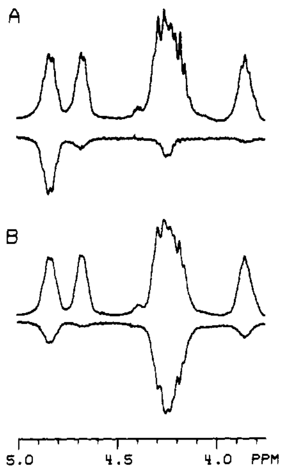

Figure 1. Nuclear Overhauser enhancements in *cyclo*(Phe-Pro-D-Ala)$_2$ in sulfolane, 30 °C. Difference spectra are the lower curves. (A) Irradiation into H^{α}_{Phe}(cis) at 4.84 ppm, showing NOE of H^{α}_{Pro}(cis) and transfer of saturation to H^{α}_{Phe}(trans). (B) Irradiation of H^{α}_{Pro}(cis) at 4.28 ppm and into overlapping H^{α}_{Pro}(trans) and H^{α}_{Ala}(trans) showing NOE of H^{α}_{Phe}(cis). Effect on H^{α}_{Ala}(cis) may be saturation transfer from H^{α}_{Ala}(trans); no NOE is anticipated.

reflections with $E > 1.75$ and three hand-picked origin-defining reflections gave an E map that revealed the positions of 88 or 92 non-hydrogen atoms of the two peptide molecules. The remaining 4 atoms of the peptide molecules and 8 water molecules were obtained from successive weighted Fourier maps.

A structure factor calculation with 100 atoms having an isotropic temperature factor of 4.7 Å^2 gave an initial R factor of 26.9%. A few cycles of block-diagonal least-squares refinement dropped the R factor to 13.3%. At this stage all 100 atoms were treated anisotropically and a few cycles of refinement brought the residual down to 0.077. Hydrogen positions were calculated and were included in the refinement. The final R factor for all 7765 reflections was 0.059.

NMR Measurements. NMR data from dimethyl sulfoxide and tetramethylene sulfone solutions were obtained by using a Nicolet NT spectrometer system operating at 300 MHz for protons. Sixteen K words of data were employed for a 4-kHz sweep width. Proton resonance assignments were made in the usual manner by decoupling and solvent variation (dimethyl sulfoxide–tetramethylene sulfone) experiments. Carbon resonance assignments were made on the basis of chemical shifts.[12] Concentrations were about 10 mM for protons and 50 mM for carbon measurements. Two cis/all-trans ratios were determined from areas of the Ala methyl resonances in fully relaxed spectra.[2] The dominant form was identified from carbon spectra.

Interproton nuclear Overhauser enhancements (NOE) were measured by using a 2-s presaturation period followed by a 90° observe pulse and acquisition with the decoupler power off. T_1 of all of the proton resonances in both two-cis and all-trans forms had been determined to be less than 0.4 s in dimethyl sulfoxide. Transformed spectra were subtracted from spectra in which H_2 was set in an interval between resonances. Minimal decoupler power was used to avoid saturation of the adjacent resonances. Areas of the difference spectra were used to estimate the enhancements; all enhancements observed were negative. An example of the NOE measurements is given in Figure 1.

Materials. Tetramethylene-d_8 sulfone, 98% isotopic enrichment, was obtained from Merck (Isotopes) and dimethyl-d_6 sulfoxide (99.96%) from Aldrich.

Results and Discussion

X-ray Crystallography. The final atomic parameters are listed in Table I. Figure 2 shows the numbering scheme used. Tables IIa and IIb give the bond lengths and angles in the two independent peptide molecules. The average standard deviations in bond lengths and angles are 0.003 Å and 0.3°, respectively. The agreement among comparable bond lengths and angles in the two crystallographically independent molecules is satisfactory, and

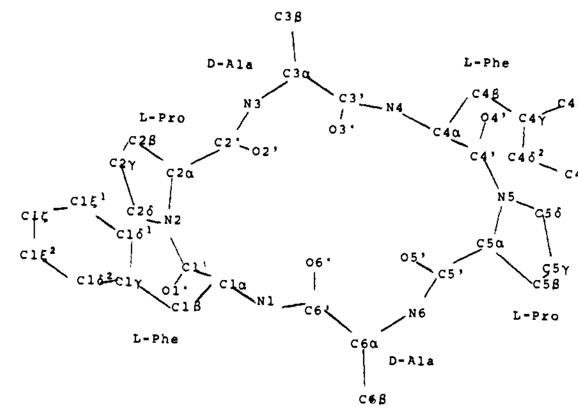

Figure 2. Numbering scheme used for (Phe-Pro-D-Ala)$_2$.

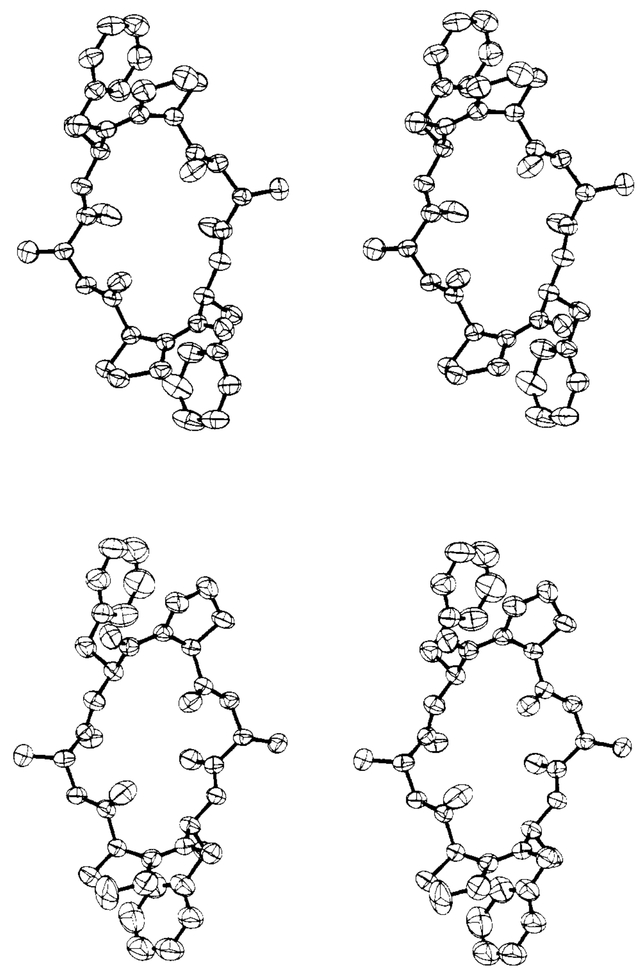

Figure 3. Stereodrawing showing the conformation of the two molecules of PPA2.

the bond lengths and angles are fairly similar to those reported in the literature.[15]

The conformations of the two peptide molecules are shown in Figure 3 (ORTEP[13] drawing), and observed torsional angles are listed in Table III. Both molecules have near twofold symmetry. All L-Phe-L-Pro peptide bonds are cis, and they show considerable deviations from planarity, with ω values varying between −3° and −21°. Comparable nonplanarity in cis peptide bonds has already been noted in the structure of the Mg^{2+} complex of *cyclo*(Gly-L-Pro-L-Pro)$_2$.[14] In the present two-cis structures there are none of the internal hydrogen bonds or β turns that have been observed

(11) Main, P.; Hull, S. E.; Lessinger, L.; Germain, G.; Declercq, J.-P.; Woolfson, M. M.; MULTAN 80, 1980—a system of computer programs for the automatic solution of crystal structures from X-ray diffraction data, Universities of York and Louvain.

(12) Howarth, O. W.; Lilley, D. M. J. *Prog. Nucl. Magn. Spectrosc.* **1977**, *12*, 1–40.

(13) Johnson, C. K., ORTEP, 1965, Oak Ridge National Laboratory Report ORNL-3796.

(14) Karle, L. I.; Karle, J. *Proc. Natl. Acad. Sci. U.S.A.* 1981, *78*, 681–685.

Table I. Fractional Coordinates (×10^5) and Their Esd's

name	*x*	*y*	*z*	B_{eq},[a] Å^2	name	*x*	*y*	*z*	B_{eq},[a] Å^2
		Molecule A					Molecule B		
N1	27493 (10)	−1078 (22)	20057 (8)	4.06	N1	53946 (10)	−40998 (22)	43437 (8)	4.00
C1α	30361 (11)	1766 (24)	14121 (9)	3.85	C1α	55259 (12)	−37905 (25)	36929 (10)	4.18
C1′	32985 (10)	−12430 (25)	11552 (10)	3.97	C1′	57457 (11)	−51816 (24)	33927 (10)	3.89
O1′	37085 (10)	−20125 (22)	14954 (9)	5.21	O1′	61711 (10)	−60021 (23)	36855 (9)	5.15
N2	31177 (10)	−15877 (21)	5616 (9)	3.99	N2	55193 (10)	−54053 (23)	27968 (9)	4.46
C2α	26558 (11)	−7744 (24)	1052 (9)	3.80	C2α	49396 (11)	−46474 (26)	24290 (10)	4.16
C2′	18663 (11)	−10948 (22)	1656 (9)	3.62	C2′	42114 (12)	−50964 (25)	26416 (10)	4.13
O2′	16598 (10)	−22219 (22)	3809 (12)	5.90	O2′	41507 (14)	−60352 (34)	30211 (14)	8.94
N3	14219 (9)	−501 (20)	−596 (9)	3.79	N3	36515 (10)	−43808 (22)	23754 (9)	4.22
C3α	6455 (10)	−1868 (23)	−718 (9)	3.62	C3α	29325 (11)	−46303 (25)	25572 (11)	4.33
C3′	3861 (11)	5937 (23)	4915 (10)	3.79	C3′	27982 (11)	−37314 (24)	31210 (10)	3.89
O3′	5210 (12)	18924 (22)	5773 (9)	6.27	O3′	29903 (10)	−24495 (20)	31654 (9)	5.09
N4	−183 (10)	−1693 (21)	8437 (9)	4.04	N4	24329 (11)	−43830 (23)	35447 (9)	4.61
C4α	−3391 (11)	4461 (24)	13766 (9)	3.85	C4α	22275 (12)	−36847 (25)	41136 (10)	4.16
C4′	−6337 (11)	−7947 (23)	17417 (9)	3.65	C4′	20374 (11)	−48614 (25)	45520 (10)	4.10
O4′	−10184 (10)	−17036 (22)	14584 (8)	5.02	O4′	16427 (12)	−58706 (24)	43609 (10)	5.79
N5	−5096 (9)	−8300 (20)	23572 (8)	3.61	N5	22490 (9)	−47206 (21)	51614 (8)	3.86
C5α	−54 (10)	731 (23)	27447 (9)	3.59	C5α	28331 (11)	−37994 (23)	54360 (9)	3.73
C5′	7747 (10)	−3379 (22)	26550 (9)	3.44	C5′	35557 (11)	−42720 (23)	52280 (9)	3.68
O5′	9339 (9)	−14820 (20)	24235 (9)	4.96	O5′	36197 (10)	−52835 (22)	48736 (9)	5.39
N6	12561 (9)	6516 (20)	28726 (8)	3.65	N6	41152 (9)	−34858 (21)	54709 (8)	3.90
C6α	20220 (10)	4052 (23)	28512 (9)	3.64	C6α	48367 (10)	−37773 (23)	53019 (9)	3.74
C6′	22465 (11)	7377 (24)	22052 (10)	3.98	C6′	49068 (11)	−33540 (24)	46270 (10)	3.87
O6′	20137 (13)	17880 (28)	19064 (11)	7.96	O6′	45512 (11)	−23622 (23)	43720 (9)	5.57
C1β	36791 (14)	12544 (31)	15047 (12)	5.15	C1β	61428 (16)	−26756 (31)	36849 (12)	5.79
C1γ	39481 (12)	16256 (26)	8777 (11)	4.51	C1γ	63618 (16)	−23536 (31)	30385 (13)	5.86
C1δ^1	36434 (14)	27418 (28)	5234 (13)	5.03	C1δ^1	60078 (21)	−13654 (40)	26477 (17)	7.19
C1ξ^1	38597 (17)	30325 (32)	−633 (14)	5.94	C1ξ^1	62286 (26)	−11470 (51)	20328 (20)	8.88
C1ζ	43873 (17)	22105 (35)	−3006 (14)	6.23	C1ζ	67924 (23)	−19158 (66)	18512 (19)	9.19
C1ξ^2	46956 (14)	10863 (34)	566 (15)	6.19	C1ξ^2	71563 (21)	−28797 (60)	22292 (18)	8.59
C1δ^2	44811 (13)	7930 (31)	6396 (13)	5.28	C1δ^2	69362 (18)	−31031 (45)	28293 (15)	7.01
C2β	28864 (14)	−13486 (34)	−5195 (12)	5.37	C2β	50368 (17)	−51626 (49)	17603 (13)	6.85
C2γ	30915 (19)	−29043 (37)	−3769 (15)	6.80	C2γ	54602 (31)	−64502 (75)	18186 (20)	11.87
C2δ	34259 (15)	−29017 (29)	2989 (14)	5.61	C2δ	57834 (18)	−66451 (37)	24589 (16)	6.90
C3β	2927 (13)	5277 (31)	−6585 (11)	4.89	C3β	23771 (14)	−42554 (42)	20116 (14)	6.17
C4β	−9658 (13)	14597 (26)	11575 (10)	4.57	C4β	15466 (15)	−27311 (32)	39705 (12)	5.42
C4γ	−13327 (12)	20761 (25)	16963 (10)	4.21	C4γ	12520 (13)	−21301 (29)	45404 (12)	5.14
C4δ^1	−10396 (15)	32119 (28)	20404 (12)	5.38	C4δ^1	15464 (20)	−9198 (42)	48342 (21)	7.75
C4ξ^1	−13782 (23)	37597 (34)	25375 (15)	7.16	C4ξ^1	12774 (31)	−3684 (59)	53816 (25)	10.03
C4ζ	−20104 (20)	31686 (37)	26858 (15)	7.58	C4ζ	7031 (25)	−10116 (71)	56065 (23)	10.18
C4ξ^2	−23027 (15)	20285 (35)	23481 (14)	6.19	C4ξ^2	3966 (19)	−22109 (59)	53135 (18)	9.01
C4δ^2	−19651 (13)	14765 (29)	18538 (12)	5.01	C4δ^2	6739 (16)	−27706 (40)	47833 (15)	6.51
C5β	−1917 (12)	−3026 (31)	34141 (10)	4.79	C5β	28051 (14)	−40125 (34)	61473 (11)	5.52
C5γ	−4433 (13)	−18631 (31)	33609 (11)	5.09	C5γ	21186 (16)	−47447 (41)	62121 (13)	6.49
C5δ	−8385 (12)	−19637 (26)	27156 (11)	4.46	C5δ	19478 (15)	−56161 (31)	56313 (12)	5.52
C6β	24389 (15)	13474 (40)	33262 (13)	6.21	C6β	53742 (12)	−29310 (31)	57416 (11)	4.79
							Solvent Molecules		
					OW1	90625 (14)	−13667 (25)	84509 (13)	7.20
					OW2	4488 (13)	−44159 (24)	24064 (12)	6.40
					OW3	81881 (18)	−2473 (31)	−4715 (13)	7.84
					OW4	7450 (15)	−66202 (25)	33048 (12)	6.76
					OW5	28430 (45)	20055 (66)	48412 (46)	16.28
					OW6	20120 (11)	26675 (24)	95471 (11)	5.93
					OW7	56745 (28)	39575 (60)	68926 (31)	12.47
					OW8	34535 (17)	−7347 (34)	46955 (29)	11.22

[a] $B_{eq} = (8\pi^2(U_{11} + U_{22} + U_{33}))/3.0$.

in crystal structures of other *cyclo*(Xxx-Pro-Yyy)$_2$ peptides, where all of the peptide bonds have been trans.[6-8]

The backbone torsional angles show some significant differences for corresponding residues within and between the hexapeptide molecules. The nonplanarity of the cis peptide bonds in molecule A is less (−3° and −12°) than that in molecule B (−16° and −21°). The prolines show variations as well. In molecule A both proline rings are C$^\gamma$-endo, while in B one is endo and the other exo. In spite of the individual variation in torsional angles, the overall backbone conformations of the two molecules are quite similar, which suggests that the general conformation adopted by the peptide ring in the crystal is a stable one, not strongly determined by the environment.

Figure 4 shows the crystal packing. There are four peptide molecules and 16 water molecules in the unit cell. The hydrophobic residues (shaded) tend to segregate to form hydrophobic and hydrophilic channels in the crystal. The hydrophilic channels are occupied by the water molecules. The hydrogen bond distances are tabulated in Table IV and the hydrogen bonding scheme is shown in Figure 5. The water molecules are all hydrogen bonded to at least one peptide carbonyl oxygen. Nine of the 12 carbonyl oxygens are hydrogen bonded to water molecules. The carbonyl oxygens of the D-alanine residues of molecule A are bridged by one water molecule (OW1), and in B a water molecule (OW7) bridges the D-alanine carbonyls. In addition to the water hydrogen bonding there is also hydrogen bonding between one alanine N–H

Table II. Bond Lengths[a] (Å) and Angles[b] (deg) for *cyclo*(L-Phe-L-Pro-D-Ala)$_2$

	peptide A (*i*)						peptide B (*i*)						
	L-Phe (1)	L-Pro (2)	D-Ala (3)	L-Phe (4)	L-Pro (5)	D-Ala (6)	L-Phe (1)	L-Pro (2)	D-Ala (3)	L-Phe (4)	L-Pro (5)	D-Ala (6)	mean
						(a) Bond Lengths							
N*i*–C*i*α	1.455	1.460	1.458	1.459	1.465	1.458	1.474	1.465	1.455	1.467	1.469	1.456	1.462
C*i*–C*i*′	1.523	1.526	1.529	1.522	1.539	1.522	1.513	1.535	1.512	1.504	1.527	1.524	1.523
C*i*′–O*i*′	1.238	1.217	1.237	1.233	1.218	1.224	1.233	1.205	1.239	1.238	1.220	1.233	1.228
C*i*′–N*i* + 1	1.333	1.338	1.323	1.327	1.340	1.325	1.333	1.327	1.333	1.344	1.343	1.335	1.333
C*i*α–C*i*β	1.562	1.545	1.524	1.543	1.554	1.508	1.550	1.544	1.539	1.559	1.551	1.534	1.543
C*i*β–C*i*γ		1.513			1.518			1.429			1.472		1.483
C*i*γ–C*i*δ		1.534			1.519			1.468			1.498		1.505
C*i*δ–N*i*		1.479			1.469			1.467			1.460		1.469
C*i*β–C*i*γ	1.523			1.513			1.517			1.498			1.513
C*i*γ–C*i*δ^1	1.377			1.371			1.373			1.376			1.374
C*i*δ^1–C*i*ξ^1	1.388			1.389			1.438			1.419			1.409
C*i*ξ^1–C*i*ζ	1.381			1.368			1.359			1.356			1.366
C*i*ζ–C*i*ξ^2	1.388			1.367			1.350			1.376			1.370
C*i*ξ^2–C*i*δ^2	1.380			1.384			1.408			1.396			1.392
C*i*δ^2–C*i*γ	1.394			1.378			1.388			1.378			1.385
						(b) Bond Angles							
C*i* – 1′–N*i*–C*i*α	120.5	127.5	122.1	122.8	127.1	121.1	120.0	127.2	121.3	124.3	126.5	120.8	123.5
C*i*α–N*i*–C*i*δ		113.1			112.7			111.8			111.7		112.3
C*i* – 1′–N*i*–C*i*δ		119.3			119.9			120.5			121.6		120.3
C*i*′–C*i*α–N*i*	108.7	111.3	109.4	107.9	111.0	110.5	108.5	110.2	110.7	107.6	111.4	110.6	109.8
N*i*–C*i*α–C*i*β	110.1	102.5	109.6	110.6	102.4	109.9	109.1	102.4	109.8	110.8	103.6	108.9	107.5
C*i*β–C*i*α–C*i*′	109.0	110.9	108.0	108.3	110.8	109.6	109.2	112.2	109.9	107.3	111.3	110.6	109.8
C*i*α–C*i*′–O*i*′	118.9	122.8	120.1	118.7	122.4	121.8	119.5	122.6	121.3	120.2	122.8	121.8	121.1
N*i* + 1–C*i*′–C*i*α	119.5	113.9	116.3	119.8	113.9	116.1	118.0	115.2	115.8	118.6	114.4	115.1	116.4
N*i* + 1–C*i*′–O*i*′	121.5	123.2	123.5	121.4	123.7	121.8	122.3	122.3	122.8	120.9	122.8	123.0	122.4
C*i*α–C*i*β–C*i*γ		103.6			103.7			106.6			104.9		104.7
C*i*β–C*i*γ–C*i*δ		105.5			104.5			111.3			106.9		107.0
C*i*γ–C*i*δ–N*i*		103.0			104.2			104.0			101.9		103.3
C*i*α–C*i*β–C*i*γ	110.0			112.3			113.8			113.7			112.5
C*i*β–C*i*γ–C*i*δ^1	120.5			121.1			122.6			121.1			121.3
C*i*β–C*i*γ–C*i*δ^2	120.5			119.8			118.8			120.8			120.0
C*i*δ^2–C*i*γ–C*i*δ^1	119.0			119.1			118.6			118.1			118.7
C*i*γ–C*i*δ^1–C*i*ξ^1	120.7			120.5			119.8			121.1			120.5
C*i*δ^1–C*i*ξ^1–C*i*ζ	120.5			119.9			119.1			119.5			119.8
C*i*ξ^1–C*i*ζ–C*i*ξ^2	118.9			119.8			122.3			120.1			120.3
C*i*ζ–C*i*ξ^2–C*i*δ^2	120.8			120.3			118.6			120.2			120.0
C*i*ξ^2–C*i*δ^2–C*i*γ	120.2			120.2			121.6			121.0			120.8

[a] The average esd for bond length is 0.003 Å. [b] The average esd for bond angle is 0.3°.

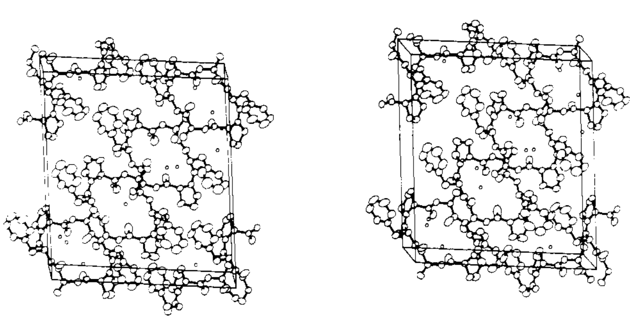

Figure 4. Stereoview of the packing of the PPA2 molecules in the crystal as viewed down the *b* axis.

of molecule B (N3) and one alanine C–O of molecule A (O1′). The carbonyl oxygen O2′ (of molecule B) is not involved in any hydrogen bonding. In the crystal the two peptide molecules have different hydrogen bonding schemes and this coupled with the packing forces might be resposible for the observed differences in the values of the conformational angles.

NMR Studies of the Conformation of *cyclo* (Phe-Pro-D-Ala)$_2$ in Solution. The spectra of the two-cis and the all-trans backbones of *cyclo*(Phe-Pro-D-Ala)$_2$ in solution are distinct. We are concerned here with the two cis form.

Coupling constant and chemical shift data of *cyclo*(Phe-Pro-D-Ala)$_2$ do not sufficiently limit the possible backbone conformations for the two-cis form, so that additional information was

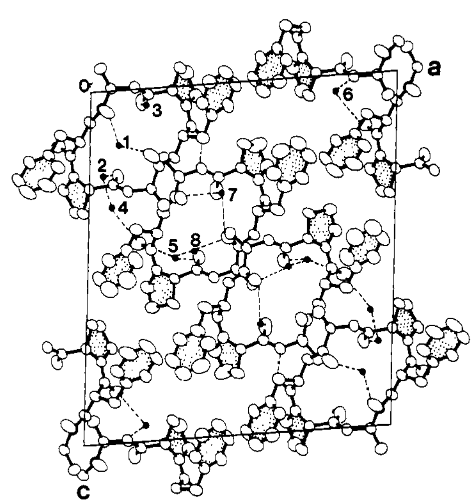

Figure 5. Hydrogen bonding scheme in the crystal as viewed down the *b* axis. The water molecules are represented by fully shaded circles and are numbered. The hydrophobic residues (shaded) tend to segregate along the 1 0 1 direction forming hydrophobic and hydrophilic channels.

sought from nuclear Overhauser enhancements. However, in Me_2SO at 25 °C no Overhauser effects within an uncertainty of 3% were observed among the backbone N–H and C^{α}–H protons. Because the absence of observable NOE's was thought likely to

Table III. Conformational Angles (deg) for *cyclo*(L-Phe-L-Pro-D-Ala)$_2$

	peptide A (i)						peptide B					
angle[a]	L-Phe (1)	L-Pro (2)	D-Ala (3)	L-Phe (4)	L-Pro (5)	D-Ala (6)	L-Phe (1)	L-Pro (2)	D-Ala (3)	L-Phe (4)	L-Pro (5)	D-Ala (6)
ϕ	−153	−83	98	−169	−70	81	−149	−71	85	−163	−63	69
ψ	133	157	−127	134	165	−144	143	174	−140	140	−179	−152
ω	−3	177	−177	−12	177	−176	−16	−176	−178	−21	−178	−179
χ^0		−19			−15			−19			−8	
χ^1	−176	32		178	31		176	19		173	−13	
χ^2	87	−35		79	−36		83	−13		81	29	
χ^3	0	23		−1	26		1	1		2	−33	
χ^4	0	−2		0	−7		−1	12		−3	26	
χ^5	0			1			0			2		
χ^6	0			−1			1			0		
χ^7	0			0			0			−1		
χ^8	0			1			−1			0		

[a] Main chain: ϕ, Ci−1′–Ni–C$i\alpha$–Ci′; ψ, Ni–C$i\alpha$–Ci′–Ni + 1; ω, C$i\alpha$–Ci′–Ni + 1–Ci + 1. Pro: χ^0, C$i\delta$–Ni–C$i\alpha$–C$i\beta$; χ^1, Ni–C$i\alpha$–C$i\beta$–C$i\gamma$; χ^2, C$i\alpha$–C$i\beta$–C$i\gamma$–C$i\delta$; χ^3, C$i\beta$–C$i\gamma$–C$i\delta$–Ni; χ^4, C$i\gamma$–C$i\delta$–Ni–C$i\alpha$. Phe: χ^1, Ni–C$i\alpha$–C$i\beta$–C$i\gamma$; χ^2, C$i\alpha$–C$i\beta$–C$i\gamma$–C$i\delta^1$; χ^3, C$i\delta^2$–C$i\gamma$–C$i\delta^1$–C$i\xi^1$; χ^4, C$i\gamma$–C$i\delta^1$–C$i\xi^1$–C$i\zeta$; χ^5, C$i\delta^1$–C$i\xi^1$–C$i\zeta$–C$i\xi^2$; χ^6, C$i\xi^1$–C$i\zeta$–C$i\xi^2$–C$i\delta^2$; χ^7, C$i\zeta$–C$i\xi^2$–C$i\delta^2$–C$i\gamma$; χ^8, C$i\xi^2$–C$i\delta^2$–C$i\gamma$–C$i\delta^1$.

Table IV. Hydrogen Bond Distances (in Å)

atom 1	atom 2	symmetry[a]	distance	esd
OW1	OW3	I (0 0 1)	3.134	0.004
OW1	O3′ (A)	II (1 −1 1	2.700	0.003
OW1	O6′ (A)	II (1 −1 1)	2.700	0.004
OW1	OW2	II (1 0 1)	2.793	0.004
OW2	O5′ (A)	I (0 0 0)	2.858	0.003
OW2	OW4	I (0 0 0)	2.831	0.003
OW3	O2′ (A)	II (1 0 0)	2.815	0.003
OW3	OW6	II (1 −1 1)	2.820	0.003
OW4	O4′ (B)	I (0 0 0)	2.794	0.003
OW4	N6 (A)	I (0 −1 0)	2.880	0.003
OW5	OW8	I (0 0 0)	2.807	0.007
OW5	O4′ (B)	I (0 1 0)	3.092	0.007
OW5	O5′ (B)	I (0 1 0)	2.894	0.006
OW6	O4′ (A)	II (0 0 1)	2.790	0.003
OW6	N3 (A)	I (0 0 1)	2.900	0.003
OW7	O3′ (B)	II (1 0 1)	2.832	0.006
OW7	O6′ (B)	II (1 0 1)	2.982	0.007
OW8	O6′ (B)	I (0 0 0)	2.689	0.004
N3 (B)	O1′ (A)	I (0 0 0)	2.904	0.003
N6 (B)	O1′ (B)	II (1 0 1)	3.005	0.003

[a] Symmetry: I, x, y, z; II, $-x$, $1/2 + y$, $-z$.

be a consequence of the rotational correlation time of the peptide rather than an indication of internuclear distances, sulfolane (tetramethylene sulfone), a solvent similar to Me_2SO but more viscous, was used for additional studies. Sulfolane has about 5 times the viscosity of Me_2SO, 9.03 vs. 1.65 cP at 35 °C.[16] Solutions of the peptide in sulfolane and in 70% sulfolane/30% Me_2SO do indeed show definitive (negative) enhancements.

Table V gives conformationally significant chemical shift and coupling constant data for the two-cis form in Me_2SO and sulfolane solutions. Table VI shows the backbone proton–proton Overhauser enhancements observed in sulfolane and in 70% sulfolane/30% Me_2SO solutions.

The two-cis form of *cyclo*(Phe-Pro-D-Ala)$_2$ shows the same H^N proton resonance temperature dependences and coupling constants, the same H^α chemical shifts, and the same abnormally high field Ala β-methyl resonance (0.82 ppm) in sulfolane as in Me_2SO. The peptide is not sufficiently soluble in sulfolane for ^{13}C measurements, but these could be made on 70% sulfolane/30% Me_2SO solutions. The conformationally significant Pro C^β and C^γ chemical shifts in the mixed solvent are found to be close to those found for Me_2SO solution. These similarities indicate similar conformations for the Phe peptide in Me_2SO and sulfolane. Nuclear Overhauser enhancement data obtained from sulfolane solutions can therefore be adduced as evidence of the conformation in Me_2SO as well as in sulfolane.

The two-cis/all-trans ratio for *cyclo*(Phe-Pro-D-Ala)$_2$ is 9 in Me_2SO, 3 in 70% sulfolane/30% Me_2SO, and 1.1 in pure sulfolane. This observation is consistent with earlier findings that decreasing solvent basicity is one factor favoring the internally hydrogen bonded all-trans form of *cyclo*(Xxx-Pro-D-Yyy)$_2$ peptides.[2,4] Although sulfolane has about the same dielectric constant as Me_2SO (43.3 vs. 46.7 at 25 °C[16]), it is a considerably poorer hydrogen bond acceptor, as indicated by the heats of complex formation with *p*-fluorophenol in the pure solvents (−4.25 and −7.21 kcal/mol, respectively).[17] A related conformationally significant observation is that the H^N_{Phe} resonance of the two-cis form moves 1.4-ppm upfield on going from Me_2SO to sulfolane. Since the conformation is similar in the two solvents, this reflects transfer of a solvent-exposed proton to a poorer hydrogen bond accepting solvent.[18,19]

The observed H–N–C^α–H coupling constants are consistent with a backbone dihedral angle ϕ_{Phe} of −120 ± 15°. For $\phi_{D\text{-}Ala}$, values of −60 ± 15°, near 75°, or near 165° are all consistent with the experimental result.[20,21] The −60° region, which puts H^N and H^α of Ala s-cis, is not consistent with the small Overhauser effect on the H^α_{Ala} lines upon irradiation into the H^N_{Ala} resonances. (See footnote *b* to Table VI and the discussion below of the NOE values.)

The value of about 11 ppm for the chemical shift difference between the Pro β- and γ-carbon resonances is consistent with a cis Phe-Pro peptide bond and correlates with ψ_{Pro} near 165° or −45°.[22] A high positive value, which puts H^α_{Pro} and H^N_{Ala} nearly cis, is supported by the −20% enhancement of the H^α_{Pro} resonance when H^H_{Ala} is irradiated. Larger Overhauser effects (−30%) are observed between H^α_{Ala} and H^N_{Phe}, suggesting that ψ_{Ala} is near −120°. Finally, −30% Overhauser effects are also observed between H^α_{Pro} and H^β_{Phe}. These two protons are close when the

(15) Benedetti, E. In "Proceedings of the Fifth American Peptide Symposium"; Goodman, M., Meinhofer, J., Eds.; Wiley: New York, 1977; pp 257–273.

(16) Riddick, J. A.; Bunger, W. B. "Organic Solvents"; 3rd ed.; Wiley-Interscience: New York, 1970; pp 467–8 and 860.

(17) Arnett, E. M.; Mitchell, E. J.; Murty, T. S. S. R. *J. Am. Chem. Soc.* **1974**, *96*, 3875–3891.

(18) Pitner, T. P.; Urry, D. W. *J. Am. Chem. Soc.* **1972**, *94*, 1339–1400.

(19) Kopple, K. D.; Schamper, T. J. In "Chemistry and Biology of Peptides"; Meienhofer, J., Ed.; Ann Arbor Science Publishers: Ann Arbor, MI, 1972; pp 75–80.

(20) Ramachandran, G. N.; Chandrasekaran, R.; Kopple, K. D. *Biopolymers* **1971**, *10*, 2113–2131.

(21) DeMarco, A.; Llinas, M.; Wüthrich, K. *Biopolymers* **1978**, *17*, 637–650.

(22) Siemion, I. Z.; Wieland, T.; Pook, K.-H. *Angew. Chem., Int. Ed. Engl.* **1975**, *14*, 702–703.

Table V. Chemical Shift and Coupling Constants of Two-Cis Forms of Cyclic Hexapeptides

		cyclo(Phe-Pro-D-Ala)$_2$			*cyclo*(Leu-Pro-D-Ala)$_2$		
parameter	solvent[a]	Phe	Pro	D-Ala	Leu	Pro	D-Ala
$\delta(H^N)$[b]	D	8.38		6.94	8.45		7.03
	S	6.97		6.58			
$d\delta/dT(H^N)$	D	−0.005		−0.0002	−0.004		−0.0027
	S	−0.003		−0.0001			
J_{HNCH}	D	9.3		6.2	9.8		6.4
	S	8.7		<6[c]			
$\delta(H^\alpha)$	D	4.85	4.31	3.84	4.60	4.37	3.94
	S	4.84	4.28	3.84			
$\delta(H^\beta)$	D	3.07	(1.98	0.82[e]		*d*	1.16
		2.67	1.72)*d*				
			1.65				
$J_{H^\alpha CH^\beta}$	D	5.3, 9.3					
$\delta(C^\beta)$	D		32.2			32.3	
	70% S + 30% D		32.3				
$\delta(C^\gamma)$	D		21.0			22.1	
	70% S + 30% D		21.5				

[a] D = dimethyl-d_6 sulfoxide; S = sulfolane, tetramethylane-d_8 sulfone. [b] 25 °C. [c] Splitting not resolved. [d] Centers of β, δ multiplets; for *cyclo*(Val-Pro-D-Ala)$_2$ which is entirely in the two-cis form, these are at 2.08 (2) and 1.80 (2) ppm. *cyclo*(Leu-Pro-L-Ala) is a 1:1 mixture of two-cis and all-trans, and the pattern was not unraveled. [e] Value in tetramethylene sulfone is 0.87 ppm.

Table VI. Backbone Proton–Proton Overhauser Enhancements in the Two-Cis Form of *cyclo*(Phe-Pro-D-Ala)$_2$, 25 °C

solvent[a]	Phe H_N	Ala H_N	Phe H_α	Pro H_α	Ala H_α
S	irrad	−0.08	−0.10	−0.08	−0.30
70 % S + 30 % D	irrad	0	0.04	−0.03	−0.14
$(r^{-6}/\sum r^{-6})_{av}$			−0.07	0	0.44
S	−0.08	irrad	−0.12	−0.20	−0.12
70 % S + 30 % D	−0.0	irrad	−0.05	−0.13	−0.08
$(r^{-6}/\sum r^{-6})_{av}$			0	0.20	0.07[b]
S	−0.12	−0.12	irrad	−0.30	−0.04
70 % S + 30 % D	−0.06	−0.05	irrad	−0.19	−0.03
$(r^{-6}/\sum r^{-6})_{av}$				0.40	0
S	0.07	−0.30	−0.30	irrad	−0.10
70 % S + 30 % D	0	−0.14	−0.18	irrad	−0.07
$(r^{-6}/\sum r^{-6})_{av}$			0.56		0.0
S	−0.25	−0.18	−0.03	−0.10	irrad
70 % S + 30 % D	−0.13	−0.07	−0.02	−0.05	irrad
$(r^{-6}/\sum r^{-6})_{av}$			0	0	

[a] S = sulfolane, tetramethylene sulfone; D = dimethyl sulfoxide; $(r^{-6}/\sum r^{-6})_{av}$ is the fraction of a maximum NOE to be expected for the conformation found in the crystal. See text. Protons within 3 Å of the observed proton are included in the sum. [b] For $\psi_{D\text{-}Ala} = -60°$, $r^{-6}/\sum r^{-6}$ is calculated to be 0.26 if $\phi_{D\text{-}Ala} = -120°$ and 0.47 if $\phi_{D\text{-}Ala} = +60°$.

Phe-Pro peptide bond is cis and closest when ψ_{Phe} is near 120° as well.

Comparing the average of the four sets of backbone dihedral angles for each kind of residue in the crystal of *cyclo*(Phe-Pro-D-Ala)$_2$ with the values estimated from the solution NMR data, we have the data in Table VII.

Table V also presents for comparison Me$_2$SO data for *cyclo*(Leu-Pro-D-Ala)$_2$, which is about 50% two-cis in dimethyl sulfoxide. The H^N chemical shifts and their relative temperature sensitivities, the H-N-C$^\alpha$-H coupling constants, the H^α_{Pro} and H^α_{Ala} chemical shifts, and the C^β_{Pro} and C^γ_{Pro} chemical shifts, all conformationally sensitive observables, are quite similar for the two-cis forms of the Phe and Leu peptides in dimethyl sulfoxide. This suggests that the backbone conformation of the two-cis form of *cyclo*(Leu-Pro-D-Ala)$_2$ is similar to that of *cyclo*(Phe-Pro-D-Ala)$_2$.

Returning the NOE data for *cyclo*(Phe-Pro-D-Ala)$_2$, an approximate test of agreement between the steady state nuclear Overhauser effects and the interproton distances in the crystal can be made under some restrictive assumptions. The least valid

Table VII

	Phe		Pro		D-Ala	
	ϕ, deg	ψ, deg	ϕ, deg	ψ, deg	ϕ, deg	ψ, deg
crystal av	−158	138	−72	169	83	−141
NMR est	120 ± 15	~120		165	75/165	~−120

of these is the assumption of a rigid structure with a single correlation time for reorientation of the interproton vectors. Other assumptions are relaxation only by proton–proton dipolar interaction, which restricts the test to carbon bound protons, and negligible spin polarization effects. The effect on the resonance of proton i or irradiating proton s should then be proportional to $r_{is}^{-6}/[r_{is}^{-6} + r_{is}^{-6}]$ where n refers to the other protons contributing to the relaxation of proton i.[23] The averages of the values of this term for the four sets of internuclear distances in the crystal appear in Table VI. Protons within 3 Å of proton i were included. The proportionality between these distance ratios and the observed Overhauser effect is the maximum proton–proton NOE for a given correlation time and Larmor frequency. From the facts that zero NOE's were observed in Me$_2$SO solutions of *cyclo*(Phe-Pro-D-Ala)$_2$ and that the viscosity of sulfolane is about five times that of Me$_2$SO, an approximate effective correlation time (3×10^{-9} s) and maximum NOE (−0.85)[23] can be estimated by assuming a linear dependence of effective correlation time on viscosity and by using eq 11 of ref 23. The calculated and found values for the larger effects are in sufficient agreement, considering the sensitivity of r_{is}^{-6} to r_{is} at the 2.1–2.3-Å distances of these four interactions found in the crystal.

	calcd	found		calcd	found
$F_{H^\alpha_{Ala}}(H^N_{Phe})$	−0.37	−0.30	$F_{H^\alpha_{Pro}}(H^\alpha_{Phe})$	−0.34	−0.30
$F_{H^\alpha_{Pro}}(H^N_{Ala})$	−0.17	−0.20	$F_{H^\alpha_{Phe}}(H^\alpha_{Pro})$	−0.48	−0.30

Coupling constant and NOE data thus indicate that the average peptide backbone of the two-cis form of *cyclo*(Phe-Pro-D-Ala)$_2$ in solution is similar to the conformation found in the crystal.

It is of interest to consider the temperature sensitivities of the H^N resonances in the light of this probable solution conformation. Neither the Phe nor Ala peptide protons are at all sequestered from the solvent by the peptide backbone, according to space-filling models, and they are not involved in intramolecular hydrogen bonds. Nonetheless $d\delta/dT$ in dimethyl sulfoxide is 0.0053

(23) Glickson, J. D.; Gordon, S. L.; Pitner, T. P.; Agresti, D. G.; Walter, R. *Biochemistry* **1976**, *15*, 5721–5729.

ppm/deg for H^N_{Phe}, a value considered to indicate solvent exposure, but only 0.0002 ppm/deg for H^N_{Ala}, a value usually taken to indicate shielding from the solvent. This distinction occurs in other peptides of the *cyclo*(Xxx-Pro-D-Ala)$_2$ series. The observed temperature coefficients (Xxx/D-Ala) for analogous peptides in which Phe is replaced by the indicated Xxx residue are as follows: Xxx = Ala, 0.003/0.006, Leu, 0.004/0.0027; Val, 0.005/0.0013 and Glu(O-*t*-Bu), 0.0046/0.0024. The distinction is absent, however, in methanol: Phe, 0.003/0.0029, and Leu, 0.0055/0.0065.[24] The temperature coefficients in dimethyl sulfoxide and the much larger upfield shift of the H^N_{Phe} resonance on shifting from dimethyl sulfoxide to sulfolane do suggest that H^N_{Phe} is more exposed to dimethyl sulfoxide than is H^{α}_{Ala}. A visible difference between them is that the Ala N–H group is flanked by H^{α}_{Pro} and the Ala β-CH_3 group,

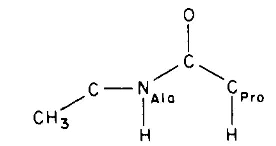

while the Phe N–H group is flanked by H^{α}_{Ala} and the Phe carbonyl oxygen

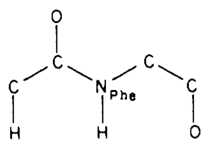

(24) Zhu, P.-P.; Go, A.; Kopple, K. D., unpublished.

Whether and how this difference explains the apparent solvent exposure is yet open to discussion.

One difference between crystal and solution conformations is apparent. Analysis of the H^{α}_{Phe}–H^{β}_{Phe} coupling constants[25] shows that one α–β rotamer with a trans pair of protons is dominant, about 0.65 mol fraction. The 0.3-ppm upfield shift of the Ala methyl protons from their normal value near 1.1 ppm (as in *cyclo*(Leu-Pro-D-Ala)$_2$, see Table V) suggests that the favored rotamer has $\chi_1 = -60°$. In the crystal $\chi_1 = 180°$; were this true in solution, large upfield shifts of some Pro protons would be expected. These were not found.

Acknowledgment. The synthesis and NMR work were supported by grants from the National Institute of General Medical Sciences, GM 26071 and GM 26071-2S1. The crystallography work was supported by National Institutes of Health Grant GM 22490 and the New York State Department of Health.

Registry No. *cyclo*(Phe-Pro-D-Ala)$_2$, 85761-33-7; H-Pro-D-Ala-OMe, 90107-57-6; *cyclo*(Leu-Pro-D-Ala)$_2$, 79546-58-0; benzyloxycarbonyl-L-phenylalanyl-L-prolyl-D-alanine methyl ester, 90107-58-7; benzyloxycarbonyl-L-phenylalanine-*N*-hydroxysuccinimide ester, 3397-32-8; benzyloxycarbonyl-L-phenylalanyl-L-prolyl-D-alanine hydrazide, 90107-59-8; L-phenylalanyl-L-prolyl-D-alanine methyl ester, 90107-60-1; benzyloxycarbonyl-L-phenylalanyl-L-prolyl-D-alanyl-L-phenylalanyl-L-prolyl-D-alanine methyl ester, 90107-61-2.

Supplementary Material Available: A listing of F_o and F_c values and hydrogen atom coordinates (41 pages). Ordering information is given on any current masthead page.

(25) Kopple, K. D.; Wiley, G. R.; Tauke, R. *Biopolymers* **1973**, *12*, 627–636.

Ferricyanide Oxidation of Dihydropyridines and Analogues

Michael F. Powell, James C. Wu, and Thomas C. Bruice*

Contribution from the Department of Chemistry, University of California at Santa Barbara, Santa Barbara, California 93106. *Received December 12, 1983*

Abstract: The reaction of the N^1-substituted dihydronicotinamides (**1–6**), *N*-benzyl-3-carbomyl-1,4-dihydropyridine (**7**), and tritiated *N*-methylacridan (**8**) with $Fe(CN)_6^{3-}$ is first order in $[Fe(CN)_6^{3-}]$ and [substrate]. The oxidations of **1–7** were followed spectrophotometrically (350 nm) while the oxidation of **8** was followed by radiometric assay. In the instances of **1**, **2**, and **8** kinetic deuterium isotope effects were determined by employing dideuterio analogues (of **1** and **2**) and deuterio–tritium substitution (for **8**). Under the conditions of $[Fe(CN)_6^{3-}] >> [PyL_2] < [Fe(CN)_6^{4-}]$, it is found that the reciprocal of the pseudo-first-order rate constant increases with increase in $[Fe(CN)_6^{4-}]$—at constant $[Fe(CN)_6^{3-}]$. This inhibition of the $Fe(CN)_6^{3-}$ oxidation of PyL_2 (L = H or D) compounds by $Fe(CN)_6^{4-}$ decreases with increase in the electronegativity of the pyridine nitrogens. This observation finds explanation in the 1e$^-$ oxidation of PyH_2 to $PyH_2^{+}\cdot$ by $Fe(CN)_6^{3-}$ and reduction of $PyH^{+}\cdot$ to PyH_2 by $Fe(CN)_6^{4-}$. A plot of the log of the rate constants (k_1) for the 1e$^-$ oxidations of a series of N^1-substituted dihydropyridines vs. the log of the rate constants (k_{HH}) for hydride transfer from N^1-substituted dihydropyridines to *N*-methylacridinium ion is linear (PyH_2 = **1**, **2**, **4**, **6**, **7**) with slope ~ 1. This finding shows that equal positive charges are generated on the pyridine nitrogen in the transition states for both the 1e$^-$ oxidation of and H^- abstraction from any of the dihydropyridines. This result establishes that such linear free energy plots do not differentiate between the mechanism of formation of $PyH_2^{+}\cdot$ and PyH^+ by 1e$^-$ and H^- oxidations. The point in the log k_1 vs. log k_{HH} plot for **8** exhibits a deviation of $>10^3$ commensurate with the greater stability of acridinyl radical cation as compared to radical cations generated from N^1-substituted dihydropyridines. The observation that the ferricyanide oxidation is first order in $Fe(CN)_6^{3-}$ and that both primary deuterium kinetic isotope effects (e.g., PyH_2 vs. PyD_2) and $Fe(CN)_6^{4-}$ inhibition are observed establishes that $PyH_2^{+}\cdot$ must exist as an intermediate. Either 1e$^-$ transfer from PyH_2 to $Fe(CN)_6^{3-}$ or H^+ transfer from $PyH_2^{+}\cdot$ to yield PyH· may be rate determining. The mechanism of Scheme I is favored in that it allows a rationalization of these observations. On increase in electron withdrawal, partitioning of $PyH_2^{+}\cdot$ species to PyH· by H^+ loss becomes favored over partitioning of $PyH_2^{+}\cdot$ to PyH_2 by reduction with $Fe(CN)_6^{4-}$. This is shown not only by the kinetically determined partition coefficient but also by the lack of inhibition of $Fe(CN)_6^{3-}$ oxidation of the electron deficient **6** by $Fe(CN)_6^{4-}$. Stabilization of the radical cation, as seen with **8**, is accompanied by marked $Fe(CN)_6^{4-}$ inhibition and a large kinetic deuterium isotope effect accompanying H^+ transfer from the radical cation. The inhibiting effect of O_2 is attributed (Scheme II) to the 1e$^-$ oxidation of PyH· to PyH^+ (not rate determining) by O_2 and reaction of the resultant $O_2^{-}\cdot$ with $PyH_2^{+}\cdot$ to regenerate O_2 and PyH_2.

Much of the controversy[1] regarding the detailed mechanism of NADH model compound (PyH,H) reduction of organic compounds that do not possess appreciable 1e$^-$ redox potentials has largely been resolved with the conclusion that H^- transfer is

0002-7863/84/1506-3850$01.50/0